Temporal transitions of spontaneous brain activity in awake rats

Zhiwei Ma, Nanyin Zhang*

Department of Biomedical Engineering, The Pennsylvania State University, University Park, PA 16802

***Address for correspondence:**

Dr. Nanyin Zhang

Hartz Family Professor

Department of Biomedical Engineering

The Huck Institutes of Life Sciences

The Pennsylvania State University

W-341 Millennium Science Complex, University Park, PA 16802, USA

Email: nuz2@psu.edu

Conflict of interest: none.

Keywords: spontaneous brain activity; resting-state functional connectivity; awake; rat; graph theory

Abstract

Spontaneous brain activity is typically investigated using resting-state fMRI (rsfMRI), which measures resting-state functional connectivity (RSFC) between brain regions. Previous rsfMRI studies mainly focused on spatial characteristics of RSFC. However, it remains elusive whether characteristic RSFC patterns temporally fluctuate in a random order, or transit in specific sequences. Here we investigated temporal transitions between characteristic RSFC patterns in awake rats. We found that transitions between RSFC patterns were highly reproducible across animals and significantly above chance, suggesting that RSFC pattern transitions were nonrandom. The global organization of RSFC pattern transitions was further examined by analyzing the RSFC pattern transition network using graph theory. Its community structure and pivotal RSFC patterns in temporal transitions were identified. Taken together, this study has revealed the temporal relationship between characteristic RSFC spatial patterns in the awake rat brain. It offers new insights into understanding the spatiotemporal dynamics of spontaneous brain activity.

Introduction

Multiple lines of evidence indicate that spontaneous brain activity plays an essential role in brain function (Raichle ME and MA Mintun 2006; Zhang D and ME Raichle 2010). For instance, intrinsic neuronal signaling consumes the vast majority of brain energy (Raichle ME 2006, 2010). Investigation of spontaneous brain activity, predominantly conducted by resting-state functional magnetic resonance imaging (rsfMRI) (Biswal B et al. 1995; Fox MD and ME Raichle 2007), has provided critical insight into understanding the intrinsic organization of the brain. Using spontaneously fluctuating blood oxygenation level-dependent (BOLD) signal measured by rsfMRI, resting-state functional connectivity (RSFC) between brain regions can be gauged by statistical interdependence of their rsfMRI signals over the period of data acquisition (Fox MD and ME Raichle 2007). Based on this quantity, multiple brain networks of functionally-related regions have been identified in both humans and animals, which convey the information of stable functional connectivity organization of the brain (Beckmann CF et al. 2005; Fox MD et al. 2005; Damoiseaux JS et al. 2006; Smith SM et al. 2009; Allen EA et al. 2011; Liang Z et al. 2011).

Conventional rsfMRI studies generally focus on steady features of RSFC by assuming that RSFC is stationary during the acquisition period. However, meaningful temporal variability of RSFC at a shorter time scale within rsfMRI scans has also been discovered (Chang C and GH Glover 2010). This initial research and its follow-up studies revealed dynamic properties of RSFC, indicating that the stationarity assumption of RSFC would be overly simplistic for understanding spontaneous brain activity (Hutchison RM, T Womelsdorf, EA Allen, et al. 2013; Preti MG et al. 2016). Indeed, using sliding window analysis and clustering methods, temporally alternating but spatially repeatable RSFC patterns have been identified (Allen EA et al. 2014). In addition, Liu and Duyn (2013) developed a method that examined instantaneous co-activations of BOLD signal at single rsfMRI frames and found that BOLD co-activation patterns well corresponded brain connectivity configurations (Liu X and JH Duyn 2013). With this method, the default mode

network, which is a single network under the assumption of stationary RSFC, can be decomposed into multiple sub-networks with distinct spatiotemporal characteristics and functional relevance (Liu X and JH Duyn 2013). Notably, the neurophysiologic relevance of dynamic RSFC has been validated in multiple studies using simultaneous electrophysiology and rsfMRI acquisitions (Tagliazucchi E et al. 2012; Chang C et al. 2013; Keilholz SD 2014).

In parallel with blossoming dynamic RSFC studies in humans, dynamic RSFC studies in animal models have also been conducted. Animals' brain preserves fundamental organizational properties as the human brain (Liang Z *et al.* 2011; Ma Z et al. 2016), and can serve as a translational model for studying complicated brain dynamics. Using either the sliding window or co-activation pattern approach, dynamic RSFC patterns have been found in both awake and anesthetized rats, as well as in anesthetized monkeys (Majeed W et al. 2011; Hutchison RM, T Womelsdorf, JS Gati, et al. 2013; Keilholz SD et al. 2013; Liang Z et al. 2015). These results suggest that dynamics in RSFC might be a general feature in mammalian brains.

Despite the critical advancement, aforementioned studies have mainly focused on the spatial characteristics of RSFC dynamics. However, the temporal relationship between RSFC patterns is still unclear. Particularly, it remains elusive whether characteristic brain connectivity patterns fluctuate in a random order, or evolve in specific temporal sequences (Majeed W *et al.* 2011; Zalesky A et al. 2014; Mitra A et al. 2015; Preti MG *et al.* 2016). Lack of such information highlights a gap in elucidating the temporal relationship between separate brain connectivity configurations, and thus hinders the comprehensive characterization of spatiotemporal dynamics of spontaneous brain activity.

To address this issue, in the present study we studied the temporal transitions of intrinsic brain activity in the awake rat brain. We first obtained a comprehensive set of characteristic RSFC patterns in the awake rat brain (Ma Z *et al.* 2016), and used them as the reference. To study the temporal relationship between these characteristic RSFC patterns, we employed the notion that

BOLD co-activation patterns in single rsfMRI frames well correspond to their RSFC patterns (Liu X et al. 2013; Liu X and JH Duyn 2013). Based on this notion, each rsfMRI frame was corresponded to one of the 40 reference RSFC patterns that had the highest spatial similarity to the BOLD co-activation pattern of the frame. This step generated a time series of RSFC patterns for each rsfMRI run. Temporal transitions between every pair of RSFC patterns were then counted, which generated a RSFC pattern transition network. A weighted direct graph, which characterized the RSFC pattern transition network, was constructed, and its topological features were studied using graph theory analysis. RSFC patterns that were pivotal in temporal transitions were further identified.

Materials and methods

Animals

41 Long-Evans (LE) adult male rats were used. Data from 31 rats were also used in another study (Ma Z *et al.* 2016) and were reanalyzed for the purpose of the present study. All rats were housed in Plexiglas cages with controlled ambient temperature (22-24 °C) and maintained on a 12 h light:12 h dark schedule. Food and water were provided ad libitum. The experiment in the present study was approved by the Institutional Animal Care and Use Committee (IACUC) at the Pennsylvania State University.

MRI experiments

Rats were acclimated to the MRI environment for seven days following the procedures described in (Zhang N et al. 2010; Liang Z *et al.* 2011, 2012, 2012, 2014; Gao YR et al. 2016) to minimize motion and stress. For the setup of awake animal imaging, the rat was first briefly anesthetized with 2-3% isoflurane and restrained into a head holder with a built-in coil and a body tube. Isoflurane was then discontinued and the rat was placed into the magnet. All rats were fully

awake during imaging.

MRI data acquisition was conducted on a Bruker 7T small animal MRI scanner (Billerica, MA). Anatomical MRI images were acquired using a T1-weighted rapid imaging with refocused echoes (RARE) sequence with the following parameters: repetition time (TR) = 1500 ms; echo time (TE) = 8 ms; matrix size = 256 × 256; field of view (FOV) = 3.2 × 3.2 cm^2; slice number = 20; slice thickness = 1 mm; RARE factor = 8. Resting-state fMRI images were acquired using a T2*-weighted gradient-echo echo planar imaging (EPI) sequence with the following parameters: TR = 1000 ms; TE =15 ms; matrix size = 64 × 64; FOV = 3.2 × 3.2 cm^2; slice number = 20; slice thickness= 1 mm. 600 EPI volumes were acquired for each run, and two to four runs were acquired for each animal.

Image preprocessing

Detailed description of the image preprocessing pipeline can be found in (Ma Z *et al.* 2016) and is briefly summarized as follows. Relative framewise displacement (FD) (Power JD et al. 2012) of rat brain EPI images were calculated, and EPI volumes with FD > 0.2 mm and their immediate temporal neighbors were removed (1.75% of total rsfMRI volumes). The first 10 volumes of each rsfMRI run were also removed to warrant a steady state of magnetization. Brain normalization to a standard rat brain was performed using Medical Image Visualization and Analysis (MIVA, http://ccni.wpi.edu/). Head motion correction was conducted using SPM12 (http://www.fil.ion.ucl.ac.uk/spm/). In-plane spatial smoothing was carried out using a Gaussian filter (FWHM = 0.75 mm). Nuisance regression was performed with the regressors of three translational and three rotation motion parameters estimated by SPM as well as white matter and ventricle signals. Band-pass filtering was performed with the frequency band of 0.01–0.1 Hz.

Characteristic RSFC patterns

To obtain a comprehensive set of characteristic RSFC spatial patterns in the awake rat brain, we used a RSFC-based whole-brain parcellation scheme (40 parcels) we previously published (Ma Z *et al.* 2016). In this scheme, voxels with similar RSFC patterns were grouped together, so that RSFC patterns were similar within parcels but dissimilar across parcels (Ma Z *et al.* 2016). As a result, these 40 characteristic RSFC patterns presented a comprehensive set of RSFC patterns in the awake rat brain (see Supplemental Information).

All characteristic RSFC patterns were respectively obtained using seed-based correlational analysis with each parcel as the seed. Specifically, mean time course averaged from all voxels within the seed region was used as the seed time course, and the Pearson cross-correlation coefficient between the seed time course and the time course of each individual brain voxel was calculated. Correlation analysis was performed for the first 540 volumes of each rsfMRI run to ensure the same degree of freedom. Correlation coefficients were then Fisher's Z-transformed. For each parcel, its group-level RSFC map was voxelwise calculated using one-sample t-test based on a linear mixed-effect model with the random effect of rats and the fixed effect of Z values in each run.

To measure the spatial similarity between reference RSFC patterns, pairwise spatial correlations between every two characteristic RSFC maps were calculated.

Temporal transitions between RSFC patterns

To analyze temporal transitions between RSFC patterns, a time sequence of framewise RSFC patterns was first obtained by corresponding each rsfMRI frame to one of the 40 reference RSFC patterns, based on the notion that BOLD co-activation patterns in single rsfMRI frames correspond to their RSFC patterns (Liu X *et al.* 2013; Liu X and JH Duyn 2013). To do so, preprocessed rsfMRI time series were first demeaned and variance normalized. The

corresponding RSFC pattern of each rsfMRI frame was identified as one of the 40 reference patterns that had the highest spatial similarity to the BOLD pattern of the frame, gauged by their spatial Pearson correlation coefficient. To ensure the correspondence between each rsfMRI frame and the RSFC pattern was statistically meaningful, we set a minimal threshold of the spatial correlation coefficient > 0.1 (p value < 10^{-13}). 89.9% of total volumes met this criterion. Frames that did not meet this criterion (10.09% of total volumes) were labeled as not corresponding to any of these 40 RSFC patterns. This step generated a time sequence of framewise RSFC patterns (i.e. BOLD co-activation patterns). In this sequence, each rsfMRI frame was denoted by a number between 1 and 40, representing its correspondence to one of the 40 characteristic RSFC patterns. The number 0 was used to denote rsfMRI frames not corresponding to any of the 40 RSFC patterns, as well as frames removed in image preprocessing (e.g. frames with large FD). In the sequence, the number of transitions between every two RSFC patterns was counted (i -> j, where $i \neq j$, $i \neq 0$ and $j \neq 0$). Transitions involving 0 (i.e., 0 -> 0, or 0 -> i, or i -> 0, where $i \neq 0$) were not counted. This procedure yielded a 40 × 40 RSFC pattern transition matrix, where its entry (i, j) represented the count of the RSFC patterns that transited from RSFC pattern i to RSFC pattern j.

Reproducibility of temporal transitions between RSFC patterns

The reproducibility of temporal transitions between RSFC patterns was assessed at both group and individual levels. At the group level, we used a split-group approach. All 41 rats were randomly divided into two subgroups with 20 rats in subgroup 1 and 21 rats in subgroup 2. The RSFC pattern transition matrix was computed for each subgroup. Entries in each matrix were normalized to the range of [0, 1], and the correlation of the corresponding off-diagonal matrix entries between the two subgroups was assessed.

It is likely that spatially more similar RSFC patterns have a higher chance to transit

between each other in both subgroups, which might inflate the reproducibility of RSFC pattern transitions between the two subgroups. To control for this effect, we regressed out the spatial similarities between reference RSFC patterns, quantified by their spatial correlation values, from the transition matrices in both subgroups and then assessed the reproducibility again.

Reproducibility of temporal transitions between RSFC patterns was also evaluated at the individual level. For each rat, its individual-level transition matrix was obtained, and a reproducibility was computed using Pearson correlation of the corresponding off-diagonal matrix entries between this individual-level transition matrix and the group-level transition matrix.

Graph theory analysis of the RSFC pattern transition network

The group-level transition matrix was thresholded to construct the RSFC pattern transition network. The p value of each entry in the transition matrix was calculated using the permutation test. Since we are only interested in transitions between two different RSFC patterns, before the permutation test, the temporal sequence of RSFC patterns was first consolidated by combining consecutive repeated appearances of the same pattern to one appearance of the pattern. For example, four consecutive appearances of Pattern ‘x’ (i.e. ‘xxxx’) was replaced by one ‘x’. This consolidated temporal sequence was then permuted 10000 times, and a transition matrix was obtained for each permuted sequence. This step generated an empirical null distribution for each off-diagonal entry in the transition matrix, and the p value of the entry was obtained accordingly. p values were further adjusted using a false-discovery rate (FDR) correction with a FDR rate of 0.05 (Genovese CR et al. 2002). Entries with insignificant p values were set to zero. All entries were then rescaled to the range of [0,1]. Finally, similarities between RSFC patterns were regressed out from nonzero entries. Using this thresholded matrix as the adjacency matrix, a graph was constructed using Gephi 0.9.1 (https://gephi.org/). In this weighted directed graph, each node represented a RSFC pattern, and an edge connecting two nodes signified an above-

chance transition between two RSFC patterns with the edge weight quantified by the normalized number of transitions.

Graph theory analysis of the RSFC pattern transition network was performed using the Brain Connectivity Toolbox (https://sites.google.com/site/bctnet/). The community affiliation of nodes in the graph was obtained by repeating the Louvain community detection algorithm (Vincent DB et al. 2008) for 1000 times to ensure a stable solution. Specifically, for each repetition, a 40 x 40 matrix was generated so that its entry (i, j) was 1 if nodes i and j were in the same community and 0 otherwise. The average of these 1000 matrices was then binarized using a threshold of 0.9, and the final inference of the community affiliation was obtained from the node affiliation of connected components in the binarized matrix (Liang Z *et al.* 2011).

To identify the hub nodes in the transition graph, local graph measures of node strength, betweenness centrality, local characteristic path length and local clustering coefficient of each node were first computed. Using these local graph metrics, hub nodes with high node strength, high betweenness centrality, short distance to other nodes, and low local clustering coefficient (Bullmore E and O Sporns 2009) were identified using the method described in (van den Heuvel MP et al. 2010). Briefly, a hub score (0 to 4) was given to each node according to the total number of the following criteria the node met: (1) upper 20 percentile in node strength; (2) upper 20 percentile in betweenness centrality; (3) lower 20 percentile in characteristic path length; and (4) lower 20 percentile in local clustering coefficient. Node met at least three criteria was defined as a hub, indicating its pivotal role in transitions between RSFC patterns.

Results

In this study, we investigated the temporal transitions between spontaneous brain activity patterns in awake rats. We first obtained a comprehensive set of characteristic RSFC spatial patterns in awake rats, using seed-based correlational analysis with parcels in a whole-brain

RSFC-based parcellation scheme as seeds. These characteristic RSFC patterns were used as the reference patterns. Subsequently, based on the notion that BOLD co-activation patterns in single rsfMRI frames correspond to their RSFC patterns (Liu X *et al.* 2013; Liu X and JH Duyn 2013), each rsfMRI frame was corresponded to one of the 40 reference RSFC patterns that had the highest spatial similarity to the BOLD co-activation pattern of the frame. This step generated a time sequence of RSFC patterns for each rsfMRI run. Temporal transitions between every pair of RSFC patterns were then counted, which provided a RSFC pattern transition matrix. A weighted directed transition network was constructed by thresholding this transition matrix, and analyzed using graph theory. A schematic illustration of these procedures is shown in Fig. 1.

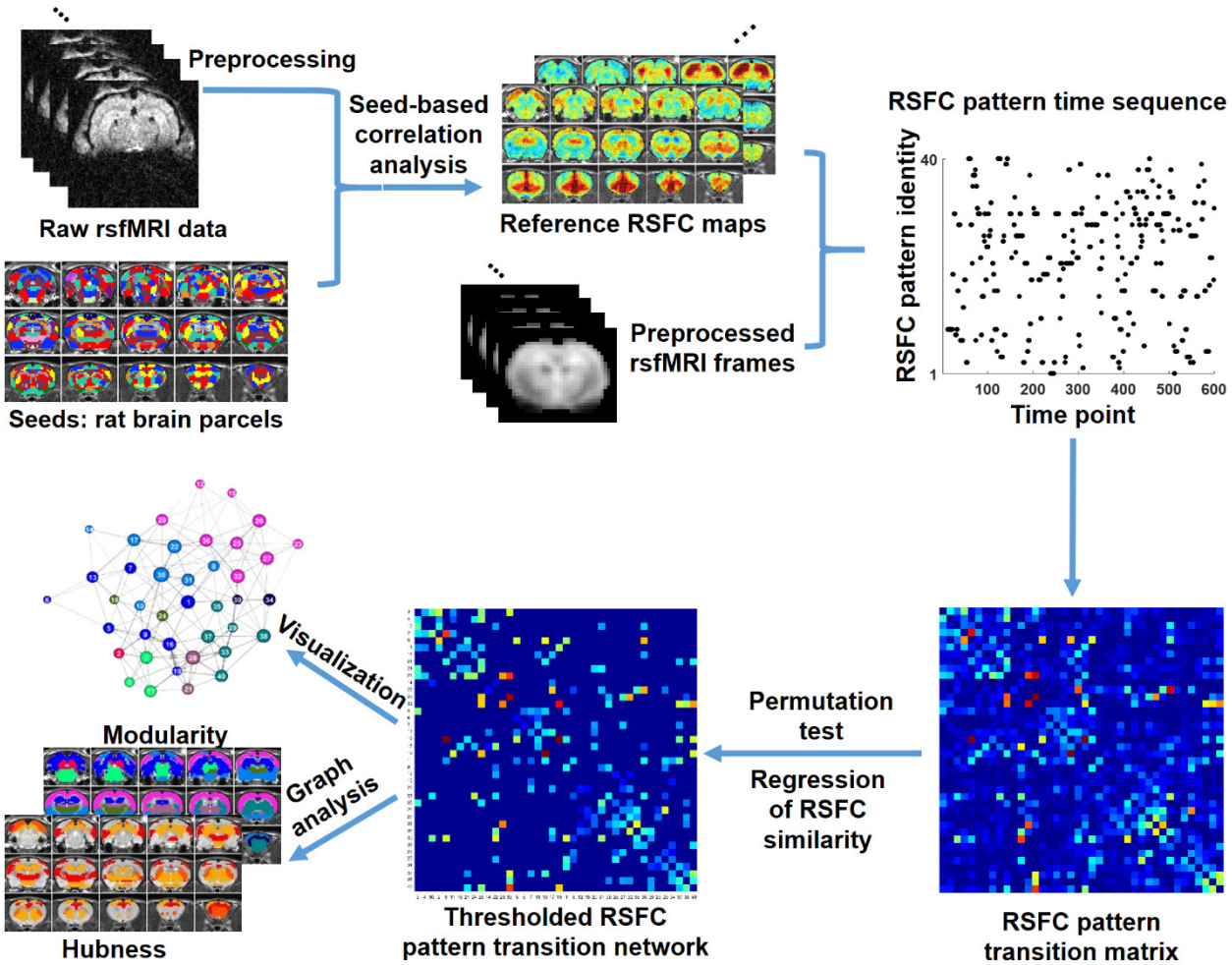

Figure 1.

Characteristic RSFC patterns in the awake rat brain

All 40 characteristic RSFC patterns are shown in Supplemental Information. As the whole-brain parcellation scheme we adopted maximized within-parcel RSFC profile similarity and minimized cross-parcel RSFC profile similarity, these 40 group-level seed-based RSFC maps represented a comprehensive survey of characteristic RSFC patterns in the awake rat brain, and thus were as the reference patterns.

Reproducible temporal transitions between RSFC patterns

We first demonstrated that temporal transitions between RSFC patterns were highly reproducible at the group level. We randomly split all rats into two subgroups and obtained the transition matrix for each subgroup. Both matrices exhibited high similarity (Fig. 2a), reflected by a significant correlation ($r = 0.86$, $p \approx 0$) between the corresponding off-diagonal entries. To control for the possibility that transitions between similar RSFC patterns may have a higher chance to occur in both subgroups, which might inflate the apparent reproducibility, we regressed out spatial similarities between reference RSFC patterns from both transition matrices. The reproducibility remained high after regression, with a significant correlation value of 0.77 ($p \approx 0$, Fig. 2b). Taken together, these results suggest that transitions between RSFC patterns are not random but follow specific temporal sequences in awake rats, and these transition sequences are not determined by the similarity between RSFC patterns.

To further examine whether RSFC pattern transitions were dominated by a small portion of rats, we assessed the reproducibility of RSFC pattern transitions for each individual animal by computing Pearson correlation between each individual-level transition matrix and the group-level transition matrix. We averaged Fisher Z-transformed correlation values across all rats, and the result indicates a reasonable individual-level reproducibility (mean (± SD) = 0.57 (± 0.14), $p \approx 0$).

These results collectively indicate that nonrandom RSFC pattern transitions are a characteristic feature in awake rats.

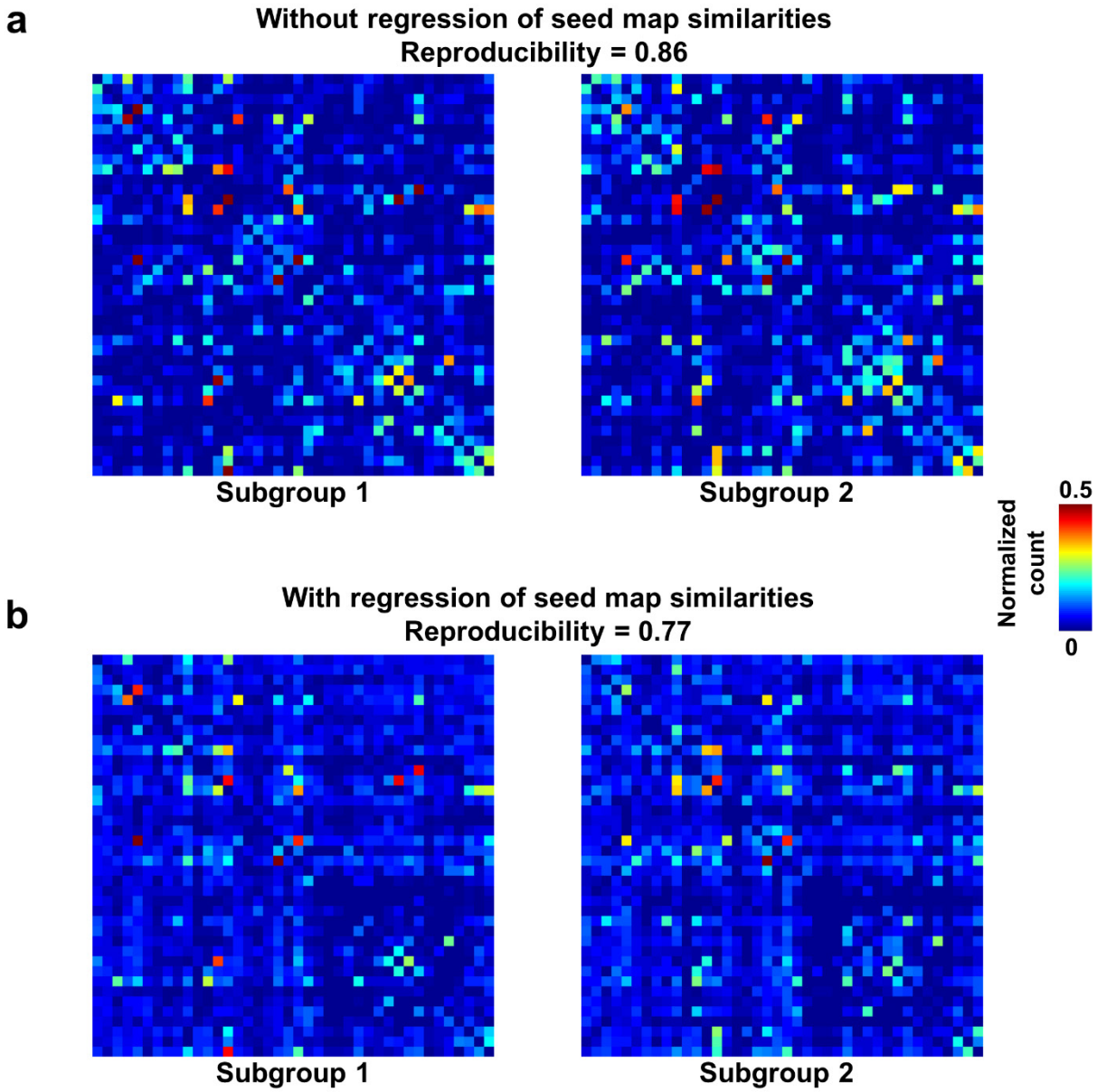

Figure 2.

Within- and between-brain system transitions

Fig. 3 shows the group-level transition matrix thresholded using a permutation test ($p <$

0.05, FDR corrected). The order of rows/columns in the transition matrix were arranged based on the brain system that the seed region of each reference RSFC pattern belonged to. RSFC pattern transitions between two successive rsfMRI frames tended to occur between RSFC patterns seeding in the same brain system, as shown by a relatively denser distribution of near-diagonal nonzero elements in the matrix (Fig. 3). In addition to prominent within-system RSFC pattern transitions in most brain systems, across-system transitions such as striatal-thalamic, striatal-somatosensory, striatal-prefrontal, striatal-hippocampal, hippocampal-amygdala, amygdala-motor transitions were observed.

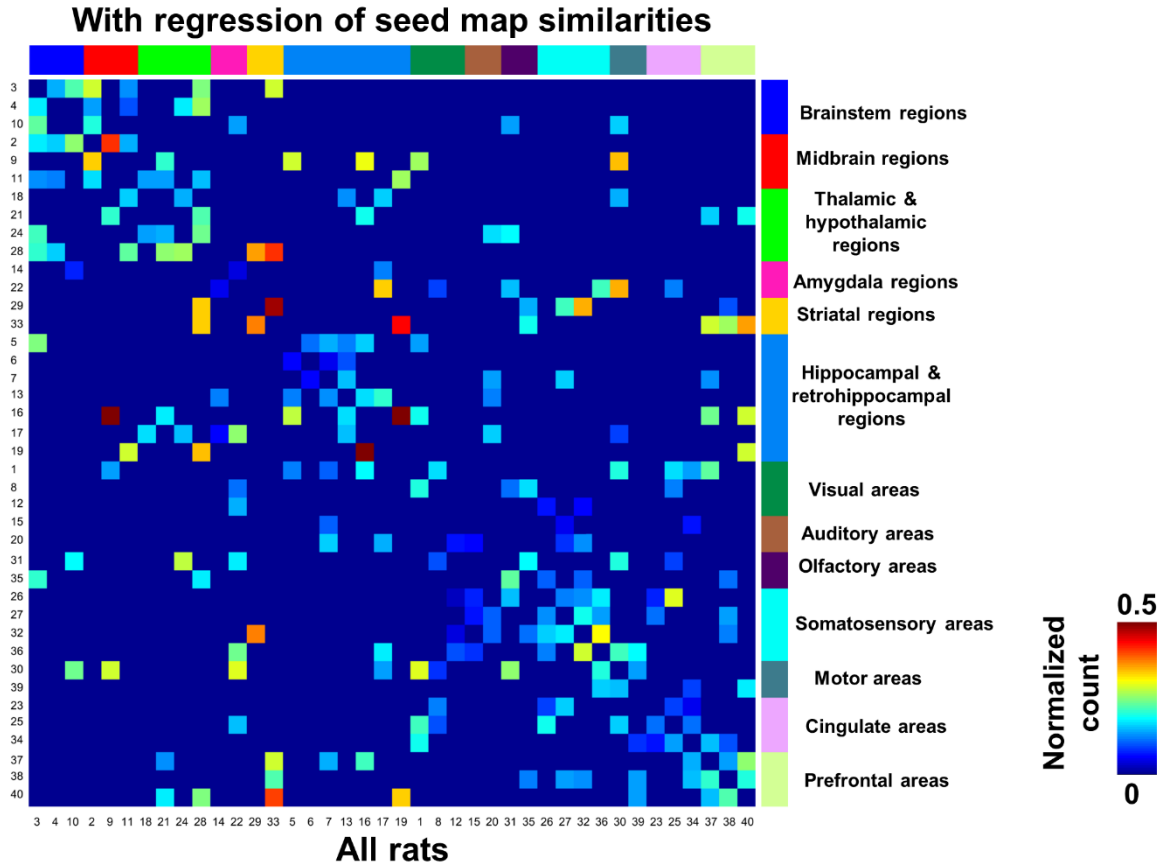

Figure 3.

Organization of the RSFC pattern transition network

A directed weighted graph of the RSFC pattern transition network was constructed based on the group-level thresholded transition matrix (Fig. 3), as visualized in Fig. 4a. The number of edges was 242, yielding a connection density of 15.5%. Using the Louvain community detection algorithm (Vincent DB *et al.* 2008), nine modules were identified in this graph. The corresponding seed regions were color coded (Fig. 4b) based on the community affiliations of nodes (i.e. RSFC patterns), and reported as follows. Module 1 primarily covered hippocampal and retrohippocampal regions as well as caudal visual areas. Module 2 included caudal midbrain regions. Module 3 was comprised of brainstem and rostral midbrain regions. Module 4 covered rostral visual areas, amygdala regions, and hypothalamic regions as well as motor and olfactory areas. Module 5 was dominated by auditory and somatosensory areas. Module 6 captured posterior ventral thalamic regions. Module 7 included anterior thalamic regions. Module 8 covered striatal regions and prefrontal areas. Module 9 mainly included anterior cingulate cortex. Regions within the same system usually fell into the same community, again indicating transitions between RSFC patterns frequently occurred between the RSFC patterns whose seeds were within the same brain system. However, several different systems were included in the same modules, which suggest the importance of across-system transitions.

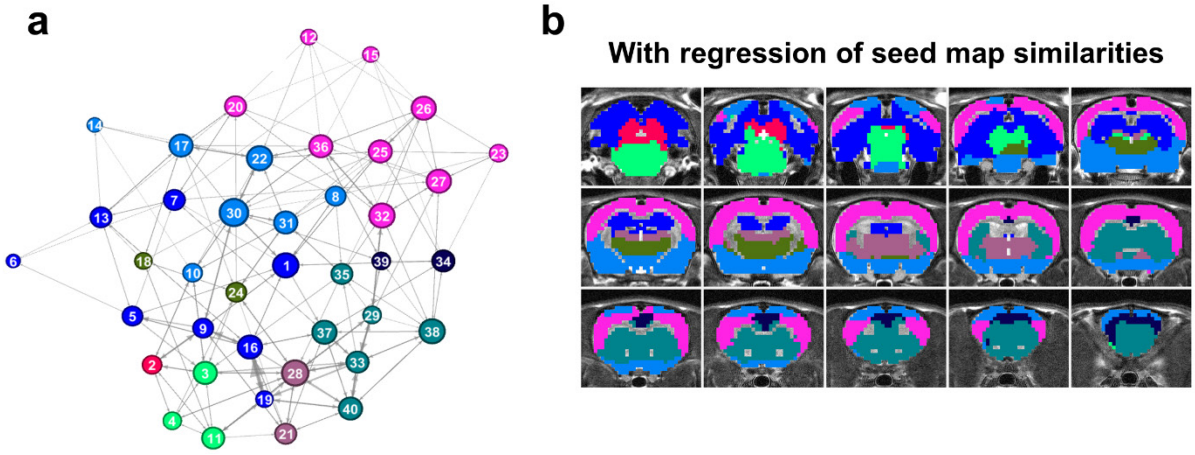

Figure 4.

By examining the node-specific graph measures of node strength, betweenness centrality, characteristic path length and local clustering coefficient, hub nodes (i.e. pivotal RSFC patterns) in the graph were identified. Fig. 5 shows seed regions of RSFC patterns with hub score ≥ 1, color coded based on the hub score. Six RSFC patterns with the hub score ≥ 3 were identified as hubs. The seed regions of these hub RSFC patterns included: the retrosplenial cortex, dorsal superior and inferior colliculi, hippocampus, anterior ventral thalamus, striatum and motor cortex.

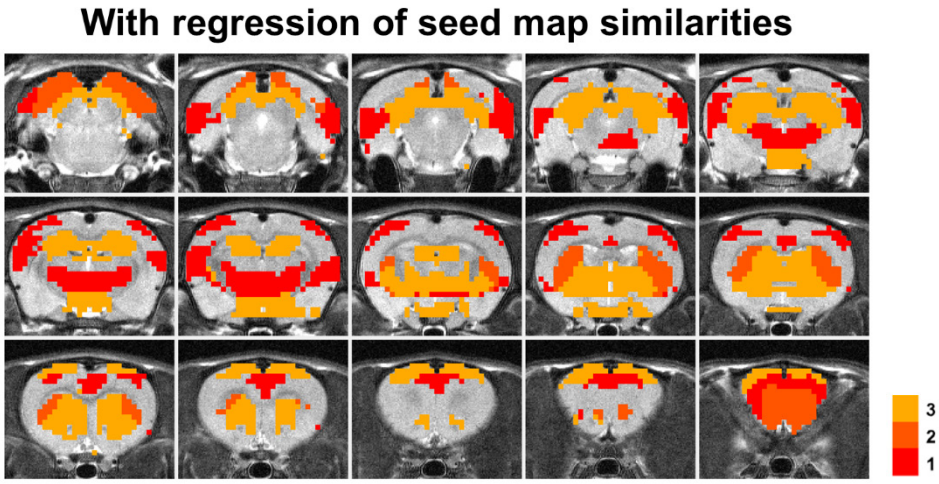

Figure 5.

Fig. 6 shows RSFC pattern transitions of four representative hubs. The pivotal role of these four hubs in RSFC pattern transitions was prominent regardless of whether or not RSFC pattern similarities were regressed out. The majority of RSFC pattern transitions between hubs and their neighboring nodes were bidirectional. Fig. 6a shows transitions of the hub RSFC pattern seeding in the superior and inferior colliculi with RSFC patterns seeding in the periaqueductal gray, hippocampus, dorsal thalamus, hypothalamus, caudal visual cortex and motor areas. Fig. 6b demonstrates transitions of the hub with the seed in the hippocampus, to/from RSFC patterns

seeding in the superior and inferior colliculi, hippocampal and retrohippocampal regions, caudal visual cortex, prefrontal and orbital cortices. Fig. 6c displays transitions between the hub RSFC pattern seeding in the anterior ventral thalamus, and the RSFC patterns seeding in the brainstem, midbrain, dorsal CA1, dorsal thalamus, posterior ventral thalamus, dorsal caudate-putamen (CPu), olfactory tubercle, and orbital cortex. Fig. 6d illustrates the transitions between the hub RSFC pattern with the seed in the ventral CPu, and the RSFC patterns of the brainstem and olfactory tubercle, as well as infralimbic, prelimbic, and orbital cortices. Taken together, these results indicate that hub RSFC patterns were centralized patterns that play a pivotal role in transitions with other RSFC patterns involving in multiple brain systems.

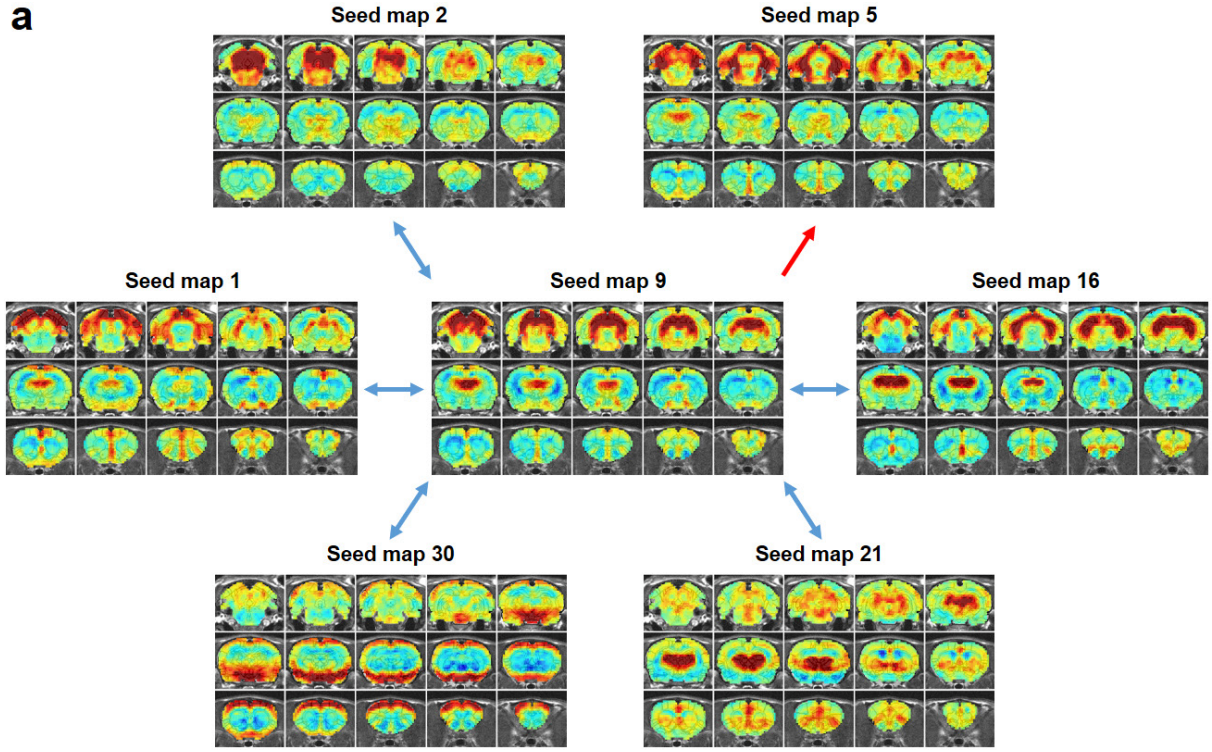

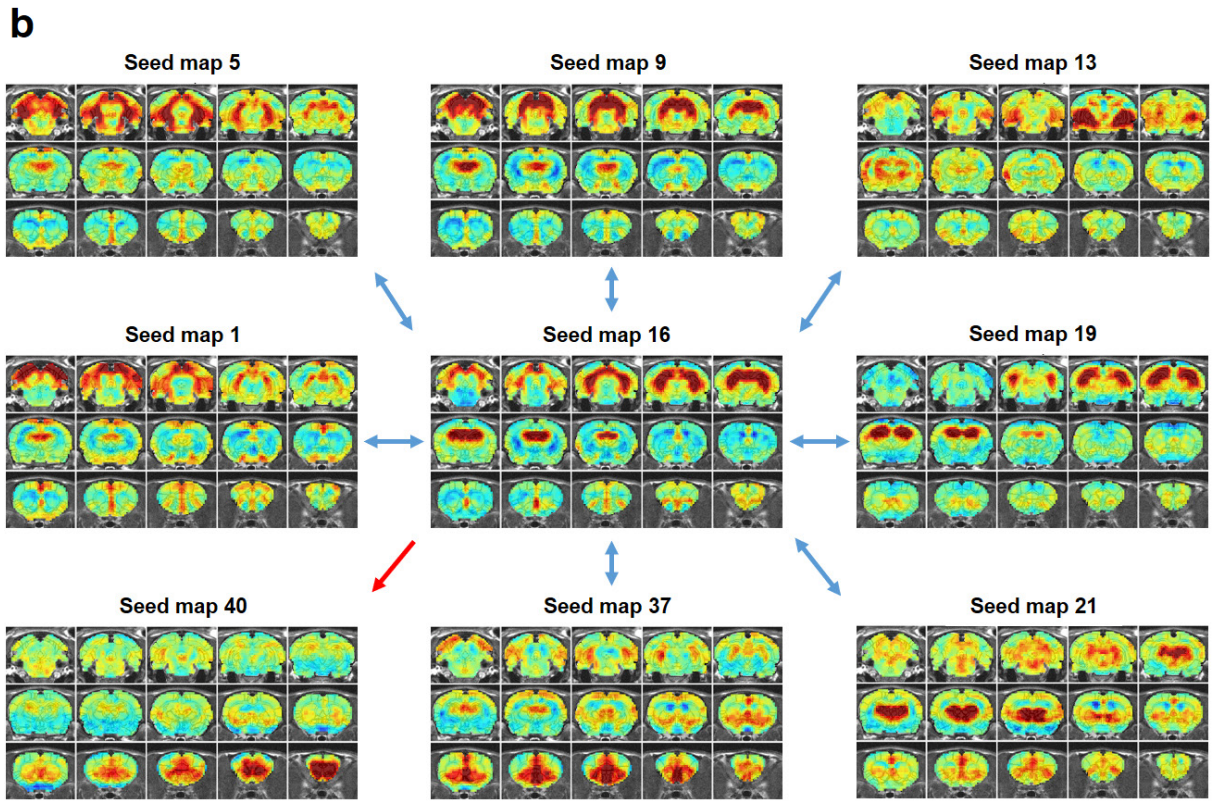

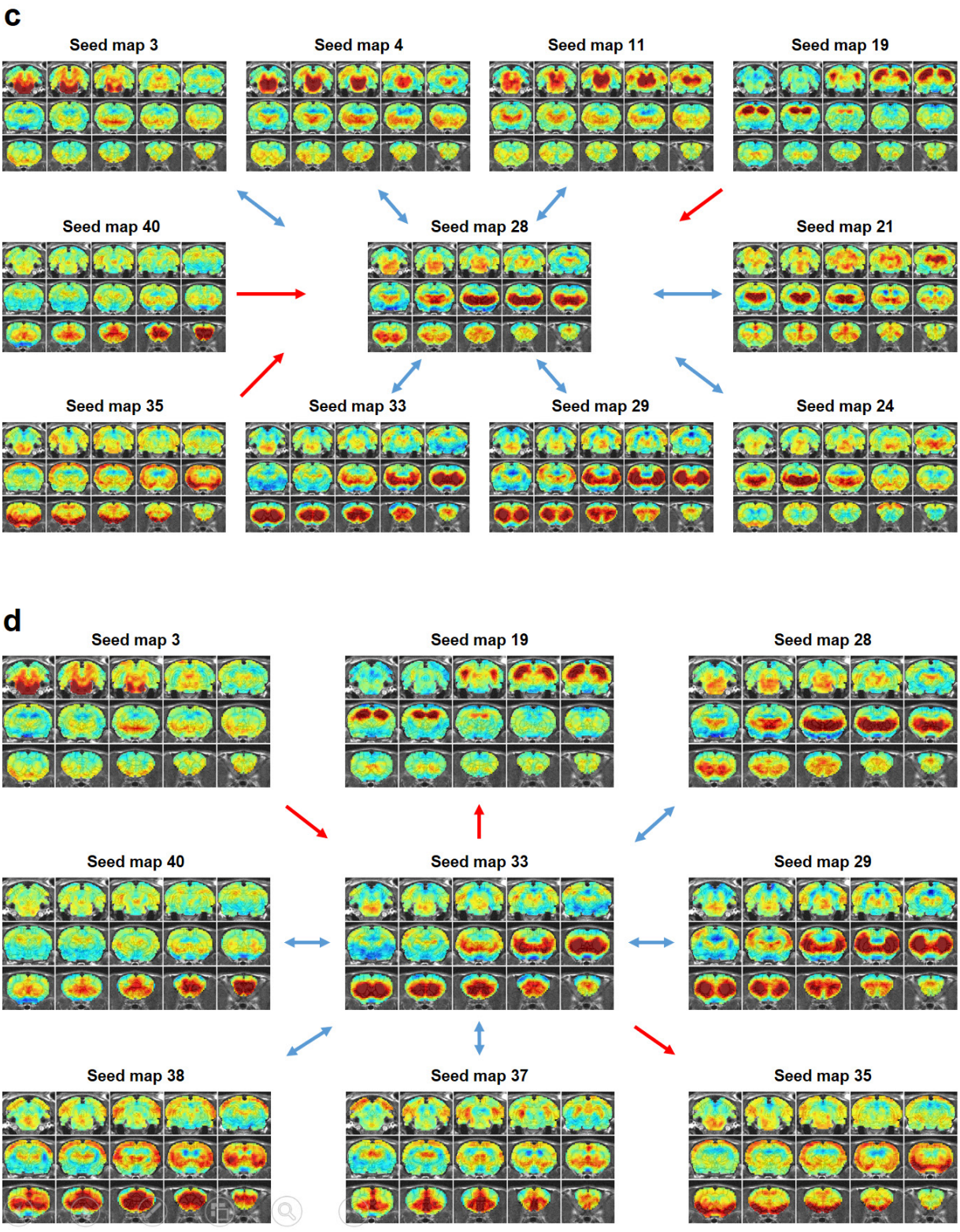

Figure 6

Discussion

In the present study, we investigated the temporal sequential transitions of intrinsic brain activity in the awake rat brain. The temporal evolution of RSFC patterns, measured by BOLD co-activation patterns in rsfMRI time series, was obtained, and the number of transitions between every two different RSFC patterns was counted. We showed that these transitions between RSFC patterns exhibited significant reproducibility across animals and significantly above chance (Figs. 2 and 3). In addition, the RSFC pattern transition network was constructed (Fig. 4a) based on the thresholded group-level transition matrix (Fig. 3), and its topological organization was evaluated in terms of community structures (Fig. 4b) and hubness (Fig. 5). Finally, the transition patterns of four representative hub RSFC patterns were demonstrated (Fig. 6). Taken together, the present study for the first time characterized the temporal sequence between successive brain connectivity configurations. It demonstrates that characteristic RSFC patterns do not fluctuate in a random manner, but follow specific orders. These results revealed the temporal relationship between characteristic RSFC spatial patterns, and has provided new insight into understanding spontaneous brain activity in the awake rat brain.

Method to elucidate the temporal relationship between characteristic RSFC patterns

Although it has been well recognized that RSFC is dynamic in nature (Hutchison RM, T Womelsdorf, EA Allen*, et al.* 2013), previous studies in this research line generally focused on revealing RSFC patterns that were temporally dynamic but spatially repeatable. Meanwhile, we have relatively sparse knowledge in the temporal relationship of different brain connectivity configurations at the resting state (Majeed W *et al.* 2011; Zalesky A *et al.* 2014). To bridge this gap, here we systematically investigated temporal transitions between different RSFC patterns.

To address this issue, we first need a comprehensive set of characteristic RSFC patterns in the awake rat brain. Since the rat brain has ~6000 brain voxels at our spatial resolution

($0.5\times0.5\times1$ mm^3), in principle we can have in total ~6000 RSFC profiles. However, elucidating temporal sequences between such a large number of RSFC patterns is not only computationally intensive, but also not necessary as many of these patterns are highly similarly to each other. To obtain a representative survey of characteristic RSFC patterns, we adopted a RSFC-based parcellation of the awake rat brain (Ma Z *et al.* 2016). In this scheme, all ~6000 voxels were clustered into 40 parcels based on the similarity of their RSFC patterns, so that brain voxels' RSFC profiles were similar within each parcel but dissimilar between parcels (Ma Z *et al.* 2016). Notably, these parcels were highly reproducible between animals and exhibited high with-parcel homogeneity (Ma Z *et al.* 2016). Therefore, RSFC patterns obtained based on these parcels are characteristic and provide a comprehensive representation all ~6000 RSFC patterns.

To examine the temporal relationship between these characteristic RSFC patterns, we adapted a recently developed method that has shown that BOLD co-activation patterns of rsfMRI frames well correspond to their instantaneous RSFC patterns (Liu X *et al.* 2013; Liu X and JH Duyn 2013). This notion has been demonstrated in both humans, as well as in awake and anesthetized rats (Liang Z *et al.* 2015). Using this notion, each rsfMRI frame was corresponded to one of 40 characteristic RSFC patterns based on their spatial similarity. This step resulted in a time sequence of RSFC patterns. Based on this sequence, we systematically examined the temporal transitions between RSFC patterns.

Nonrandom temporal transitions between RSFC patterns

Our data showed that temporal transitions between RSFC patterns were highly reproducible, reflected by significant reproducibility between randomly divided subgroups. In addition, these transitions were not dominated by a small portion of animals, evidenced by the reproducibility at the individual level. These results were consistent with previous studies showing that BOLD signal periodically propagated from lateral to medial cerebral cortex (Majeed W et al.

2009; Majeed W *et al.* 2011), indicating repeatable spatiotemporal dynamics. It should be noted that the reproducibility assessment using the split-group method relies on the assumption that RSFC pattern transitions were independent. However, transitions may have a higher chance to occur between spatially more similar RSFC patterns in both subgroups, which might artificially increase the reproducibility. To control for this factor, the similarities between RSFC patterns were regressed out in the transition matrices of both subgroups, and we found that the reproducibility of RSFC pattern transitions remained high. These data show that transitions between RSFC patterns were robust. In addition, using permutation tests, we identified a number of transitions between RSFC patterns that were statistically above chance. Taken together, these results provide strong evidence indicating that RSFC patterns do not transit between each other in a random manner, but follow specific temporal sequences.

RSFC pattern transitions within and across brain systems,

We found that transitions between RSFC patterns occurred frequently between patterns seeding within the same brain system (Fig. 3). This result might be attributed to the fact that seed regions in the same brain system typically subserve similar brain function. In addition, regions in the same brain system are usually strongly connected with each other (Liang Z et al. 2013), and thus transitions between their RSFC patterns can frequently occur.

Our data also showed prominent across-system transitions (Fig. 3). For instance, BOLD co-activations can transit between striatal regions and somatosensory/prefrontal cortical regions. We speculate that bidirectional transitions between striatal and somatosensory/prefrontal RSFC patterns might indicate the presence of both “bottom-up” and “top-down” processing between high-order cortical and low-order subcortical regions at rest. Corticostriatal projections have been identified in the rat brain (Paxinos G 2015), which can be the anatomical basis for cortical-subcortical RSFC pattern transitions. In addition, striatal to thalamic/hippocampal RSFC pattern

transitions indicate a close relationship between these subcortical regions at the resting state. As an example, strong RSFC has been found between CPu and thalamus in the rat brain (Liang Z *et al.* 2013). Taken together, these results show non-trivial spatiotemporal dynamics of spontaneous brain activity within and cross systems in the awake rat brain.

Topological organization of the RSFC pattern transition network

A graph characterizing transition network between RSFC patterns was constructed with each node representing a RSFC pattern and each edge denoting the above-chance transition relationship between the two nodes. We further investigated topological properties of this weighted directed graph in terms of its community structure and hubness. The transition network exhibited a prominent community structure evidenced by high modularity. Consistent with our observation that transitions frequently occurred between RSFC patterns seeding within the same brain system (Fig. 3), RSFC patterns whose seed regions were within the same brain system usually belonged to the same module (Fig. 4b). However, this result is not exclusive as we also observed that seeds from different systems were also grouped in the same modules, highlighting their close temporal relationship and the importance of cross-system transitions.

We also identified several hub RSFC patterns (Fig. 5) and scrutinized their transition patterns (Fig. 6). Hubs are central nodes in the graph which play a pivotal role in relation to other RSFC patterns. In consistency with our previous findings that anterior ventral thalamus is a critical hub in the rat functional brain network (Ma Z *et al.* 2016), the RSFC pattern of anterior ventral thalamus was also a hub in the network of RSFC pattern transitions. In addition, the RSFC pattern seeding in the hippocampus was identified as a hub pattern pivotal to transitions to RSFC patterns seeding in the superior and inferior colliculi, as well as the visual, prefrontal and orbital cortices. Interestingly, the hippocampus has been observed to interact with multiple cortical and subcortical regions in the form of sharp wave ripples, and the onset of such ripples were found to be controlled

by the propagating signals from the cortex to hippocampus (Molle M et al. 2006; Hahn TT et al. 2012; Roumis DK and LM Frank 2015). Although sharp wave ripples and RSFC pattern transitions involving the hippocampus might be from different signal sources, the centralized role of the hippocampus is shared by these two forms of hippocampal-cortical information flow. Further, our data revealed a hub of the RSFC pattern seeding in the ventral CPu. As a part of the striatum, CPu is linked to multiple corticostriatal projections (Paxinos G 2015), and it might play a centralized role in transitions involving multiple cortical RSFC patterns. Taken together, these data indicate that hub RSFC patterns (i.e. BOLD co-activation patterns) might play a centralized role linking multiple brain systems and might be critical for us to understand how activities from different brain systems are integrated to maintain normal brain function.

Potential limitation

One limitation of the present study is that single rsfMRI frames could exhibit features of more than one RSFC pattern. It should be noted that corresponding a rsfMRI frame to its most similar reference RSFC pattern is only an approximation for the purpose of investigating spatiotemporal dynamics of spontaneous brain activity. To mitigate this issue, we set a minimal threshold (correlation coefficient > 0.1, 10^{-13}) to remove rsfMRI frames that were not similar to any of these 40 RSFC patterns (e.g. rsfMRI frames dominated by noise), and ensured that the similarity between each rsfMRI frame and the RSFC pattern it corresponded to was statistically significant after Bonferroni correction ($p < 0.05/40834$ rsfMRI volumes $\approx 10^{-6}$). 89.9% of total rsfMRI volumes met this criterion, indicating that the reference RSFC patterns indeed captured most spontaneous brain activity patterns in the awake rat brain.

Conclusions

In conclusion, the present study investigated temporal transitions between spontaneous

brain activity patterns in the awake rat brain. The temporal sequence of framewise RSFC patterns was obtained. Reproducible transitions between RSFC patterns were identified in the sequence. Using graph theory analysis, our study further revealed community structures and hubness of the RSFC pattern transition network. This study has opened a new avenue to investigate the spatiotemporal relationship of spontaneous brain activity in the awake animal.

Acknowledgments

The present study was supported by National Institute of Neurological Disorders and Stroke Grant R01NS085200 (PI: Nanyin Zhang, PhD) and National Institute of Mental Health Grant R01MH098003 (PI: Nanyin Zhang, PhD). Part of this research was conducted using the high-performance computing resources provided by the Institute for CyberScience at the Pennsylvania State University (https://ics.psu.edu).

Conflict of interest: none.

References:

Allen EA, Damaraju E, Plis SM, Erhardt EB, Eichele T, Calhoun VD. 2014. Tracking whole-brain connectivity dynamics in the resting state. Cereb Cortex 24:663-676.

Allen EA, Erhardt EB, Damaraju E, Gruner W, Segall JM, Silva RF, Havlicek M, Rachakonda S, Fries J, Kalyanam R, Michael AM, Caprihan A, Turner JA, Eichele T, Adelsheim S, Bryan AD, Bustillo J, Clark VP, Feldstein Ewing SW, Filbey F, Ford CC, Hutchison K, Jung RE, Kiehl KA, Kodituwakku P, Komesu YM, Mayer AR, Pearlson GD, Phillips JP, Sadek JR, Stevens M, Teuscher U, Thoma RJ, Calhoun VD. 2011. A baseline for the multivariate comparison of resting-state networks. Front Syst Neurosci 5:2.

Beckmann CF, DeLuca M, Devlin JT, Smith SM. 2005. Investigations into resting-state connectivity using independent component analysis. Philos Trans R Soc Lond B Biol Sci 360:1001-1013.

Biswal B, Yetkin FZ, Haughton VM, Hyde JS. 1995. Functional connectivity in the motor cortex of resting human brain using echo-planar MRI. Magn Reson Med 34:537-541.

Bullmore E, Sporns O. 2009. Complex brain networks: graph theoretical analysis of structural and functional systems. Nat Rev Neurosci 10:186-198.

Chang C, Glover GH. 2010. Time-frequency dynamics of resting-state brain connectivity measured with fMRI. Neuroimage 50:81-98.

Chang C, Liu Z, Chen MC, Liu X, Duyn JH. 2013. EEG correlates of time-varying BOLD functional connectivity. Neuroimage 72:227-236.

Damoiseaux JS, Rombouts SA, Barkhof F, Scheltens P, Stam CJ, Smith SM, Beckmann CF. 2006. Consistent resting-state networks across healthy subjects. Proc Natl Acad Sci U S A 103:13848-13853.

Fox MD, Raichle ME. 2007. Spontaneous fluctuations in brain activity observed with functional magnetic resonance imaging. Nat Rev Neurosci 8:700-711.

Fox MD, Snyder AZ, Vincent JL, Corbetta M, Van Essen DC, Raichle ME. 2005. The human brain is intrinsically organized into dynamic, anticorrelated functional networks. Proceedings of the National Academy of Sciences of the United States of America 102:9673-9678.

Gao YR, Ma Y, Zhang Q, Winder AT, Liang Z, Antinori L, Drew PJ, Zhang N. 2016. Time to wake up: Studying neurovascular coupling and brain-wide circuit function in the un-anesthetized animal. Neuroimage.

Genovese CR, Lazar NA, Nichols T. 2002. Thresholding of statistical maps in functional neuroimaging using the false discovery rate. Neuroimage 15:870-878.

Hahn TT, McFarland JM, Berberich S, Sakmann B, Mehta MR. 2012. Spontaneous persistent activity in entorhinal cortex modulates cortico-hippocampal interaction in vivo. Nat Neurosci 15:1531-1538.

Hutchison RM, Womelsdorf T, Allen EA, Bandettini PA, Calhoun VD, Corbetta M, Della Penna S, Duyn JH, Glover GH, Gonzalez-Castillo J, Handwerker DA, Keilholz S, Kiviniemi V, Leopold DA, de Pasquale F, Sporns O, Walter M, Chang C. 2013. Dynamic functional connectivity: promise, issues, and interpretations. Neuroimage 80:360-378.

Hutchison RM, Womelsdorf T, Gati JS, Everling S, Menon RS. 2013. Resting-state networks show dynamic functional connectivity in awake humans and anesthetized macaques. Hum Brain Mapp 34:2154-2177.

Jacomy M, Venturini T, Heymann S, Bastian M. 2014. ForceAtlas2, a continuous graph layout algorithm for handy network visualization designed for the Gephi software. PLoS One 9:e98679.

Keilholz SD. 2014. The neural basis of time-varying resting-state functional connectivity. Brain Connect 4:769-779.

Keilholz SD, Magnuson ME, Pan WJ, Willis M, Thompson GJ. 2013. Dynamic properties of functional connectivity in the rodent. Brain connectivity 3:31-40.

Liang Z, King J, Zhang N. 2011. Uncovering intrinsic connectional architecture of functional networks in awake rat brain. J Neurosci 31:3776-3783.

Liang Z, King J, Zhang N. 2012. Anticorrelated resting-state functional connectivity in awake rat brain. Neuroimage 59:1190-1199.

Liang Z, King J, Zhang N. 2012. Intrinsic organization of the anesthetized brain. J Neurosci 32:10183-10191.

Liang Z, King J, Zhang N. 2014. Neuroplasticity to a single-episode traumatic stress revealed by resting-state fMRI in awake rats. Neuroimage 103:485-491.

Liang Z, Li T, King J, Zhang N. 2013. Mapping thalamocortical networks in rat brain using resting-state functional connectivity. Neuroimage 83:237-244.

Liang Z, Liu X, Zhang N. 2015. Dynamic resting state functional connectivity in awake and anesthetized rodents. Neuroimage 104:89-99.

Liu X, Chang C, Duyn JH. 2013. Decomposition of spontaneous brain activity into distinct fMRI co-activation patterns. Front Syst Neurosci 7:101.

Liu X, Duyn JH. 2013. Time-varying functional network information extracted from brief instances of spontaneous brain activity. Proc Natl Acad Sci U S A 110:4392-4397.

Ma Z, Perez P, Ma Z, Liu Y, Hamilton C, Liang Z, Zhang N. 2016. Functional atlas of the awake rat brain: A neuroimaging study of rat brain specialization and integration. Neuroimage.

Majeed W, Magnuson M, Hasenkamp W, Schwarb H, Schumacher EH, Barsalou L, Keilholz SD. 2011. Spatiotemporal dynamics of low frequency BOLD fluctuations in rats and humans. Neuroimage 54:1140-1150.

Majeed W, Magnuson M, Keilholz SD. 2009. Spatiotemporal dynamics of low frequency fluctuations in BOLD fMRI of the rat. J Magn Reson Imaging 30:384-393.

Mitra A, Snyder AZ, Blazey T, Raichle ME. 2015. Lag threads organize the brain's intrinsic activity. Proc Natl Acad Sci U S A 112:E2235-2244.

Molle M, Yeshenko O, Marshall L, Sara SJ, Born J. 2006. Hippocampal sharp wave-ripples linked to slow oscillations in rat slow-wave sleep. J Neurophysiol 96:62-70.

Paxinos G. 2015. The rat nervous system. Amsterdam: Elsevier/AP, Academic Press is an imprint of Elsevier.

Power JD, Barnes KA, Snyder AZ, Schlaggar BL, Petersen SE. 2012. Spurious but systematic correlations in functional connectivity MRI networks arise from subject motion. Neuroimage 59:2142-2154.

Preti MG, Bolton TA, Van De Ville D. 2016. The dynamic functional connectome: State-of-the-art and perspectives. Neuroimage.

Raichle ME. 2006. Neuroscience. The brain's dark energy. Science 314:1249-1250.

Raichle ME. 2010. The brain's dark energy. Sci Am 302:44-49.

Raichle ME, Mintun MA. 2006. Brain work and brain imaging. Annu Rev Neurosci 29:449-476.

Roumis DK, Frank LM. 2015. Hippocampal sharp-wave ripples in waking and sleeping states. Curr Opin Neurobiol 35:6-12.

Smith SM, Fox PT, Miller KL, Glahn DC, Fox PM, Mackay CE, Filippini N, Watkins KE, Toro R, Laird AR, Beckmann CF. 2009. Correspondence of the brain's functional architecture during activation and rest. Proc Natl Acad Sci U S A 106:13040-13045.

Tagliazucchi E, von Wegner F, Morzelewski A, Brodbeck V, Laufs H. 2012. Dynamic BOLD functional connectivity in humans and its electrophysiological correlates. Front Hum Neurosci 6:339.

van den Heuvel MP, Mandl RC, Stam CJ, Kahn RS, Hulshoff Pol HE. 2010. Aberrant frontal and temporal complex network structure in schizophrenia: a graph theoretical analysis. J Neurosci 30:15915-15926.

Vincent DB, Jean-Loup G, Renaud L, Etienne L. 2008. Fast unfolding of communities in large networks. Journal of Statistical Mechanics: Theory and Experiment 2008:P10008.

Zalesky A, Fornito A, Cocchi L, Gollo LL, Breakspear M. 2014. Time-resolved resting-state brain networks. Proc Natl Acad Sci U S A 111:10341-10346.

Zhang D, Raichle ME. 2010. Disease and the brain's dark energy. Nat Rev Neurol 6:15-28.

Zhang N, Rane P, Huang W, Liang Z, Kennedy D, Frazier JA, King J. 2010. Mapping resting-state brain networks in conscious animals. J Neurosci Methods 189:186-196.

Figure Captions

Figure 1. Schematic illustration of the data analysis pipeline.

Figure 2. Reproducibility of the RSFC pattern transition matrix. a. RSFC pattern transition matrices of subgroup 1 and 2 without the regression of similarities between RSFC patterns. b. RSFC pattern transition matrices of subgroup 1 and 2 with the regression of similarities between RSFC patterns.

Figure 3. Thresholded group-level RSFC pattern transition matrix with the regression of RSFC patterns similarities.

Figure 4. Community structures of the RSFC pattern transition network. a. Visualization of the transition network. The thresholded transition matrix in Fig. 3 was used as the adjacency matrix to generate this graph. The layout of nodes was based on a force-field algorithm (Jacomy M et al. 2014). b. Community structures. Based on the community affiliations of nodes (i.e. RSFC patterns), the corresponding seed regions within the same community were colored coded.

Figure 5. Node-specific hub scores. The seed regions of RSFC patterns were color coded according to the hub score.

Figure 6. Transition patterns of hubs. Blue arrows denote edges of bidirectional transitions between RSFC patterns. Red arrows denote edges of unidirectional transitions between RSFC patterns. Edges between neighboring nodes of hub nodes are not shown.